Strategies for using cellular automata to locate constrained layer damping on vibrating structures

C M Chia, J A Rongong and K Worden

Department of Mechanical Engineering, The University of Sheffield, Mappin Street, Sheffield, S1 3JD, UK.

Abstract

It is often hard to optimise constrained layer damping (CLD) for structures more complicated than simple beams and plates as its performance depends on its location, the shape of the applied patch, the mode shapes of the structure and the material properties. This paper considers the use of cellular automata (CA) in conjunction with finite element analysis to obtain an efficient coverage of CLD on structures. The effectiveness of several different sets of local rules governing the CA are compared against each other for a structure with known optimum coverage – namely a plate. The algorithm which attempts to replicate most closely known optimal configurations is considered the most successful. This algorithm is then used to generate an efficient CLD treatment that targets several modes of a curved composite panel. To validate the modelling approaches used, results are also presented of a comparison between theoretical and experimentally obtained modal properties of the damped curved panel.

Keywords

constrained layer, damping, cellular automata, vibration control

1 Introduction

Constrained layer damping (CLD) is a surface treatment comprising a layer of a flexible damping material sandwiched between the host structure and a stiff constraining layer. As the structure vibrates, relative in-plane motion between the host structure and the constraining layer can induce large dynamic shear strains in the damping material. This is the principal energy dissipation mechanism in CLD [1]. Effectiveness depends on a number of different parameters including material properties, layer thickness, location, surface coverage and the distribution of dynamic strain on the host structure. Over the years, many have optimised CLD for beams and plates using analytical models [2–7]. There is now an increasing desire to apply CLD efficiently to more complicated structures that are normally modelled using Finite Element (FE) analysis. The large number of design variables makes the optimisation of CLD using such models challenging with regard to computing power when using traditional search techniques. The need for a quicker solution has led researchers to consider evolutionary strategies that have included the Genetic Algorithm [8-10] and a local gradient descent approach [11].

This paper considers a different type of evolutionary strategy for locating CLD treatments on FE models of structures, namely Cellular Automata (CA) algorithms. These involve sets of simple local rules that govern interactions between cells that make up the system [12]. In a structure comprising many cells, even simple local rules can be effective in describing complicated behaviour of the overall system. The CA approach has been demonstrated in the design of lightweight load bearing structures [13–15] and in finding the optimum location of free layer damping treatments [16]. Recently, the authors demonstrated the use of CA for locating CLD treatments on a vibrating plate [17]. The motivation to locate CLD using the CA approach rather than global optimisation methods lies in the expected reduction in computation effort if suitable local rules can be applied. The local rules used, were shown to achieve near-optimum solutions for modal strain distributions that were primarily unidirectional and aligned with the FE mesh. However, for more complicated mode shapes, evolved treatments were around 30% less effective. This result highlights one of the main difficulties in using the CA approach: there is no guidance on how to choose the appropriate local rule for a given problem. To help identify the best rule for CLD, this paper examines the effectiveness of several different local rules. The best of these CA rules is then used to improve simultaneously the damping of the first four vibration modes of a curved composite

panel. As the distribution of modal strain is considerably more complicated than for a flat, isotropic plate, application to this problem provides a good opportunity for the algorithm to demonstrate its effectiveness.

2 Optimisation of CLD

There are two distinct energy dissipation mechanisms in CLD systems. The most commonly studied one is shear deformations in the viscoelastic layer. The other mechanism involves out-of-plane tension and compression of the viscoelastic material (VEM). Out-of-plane direct strains in VEM occur when the viscoelastic layer is very flexible in comparison to the constraining layer or when the mass of the constraining layer is high. Though high levels of damping can be achieved where out-of-plane deformations occur, this regime occurs in a relatively narrow (and unusual) design space – at high frequencies and mode numbers [18]. As the work presented here focuses on lower-order modes, the shear dominated mechanism is of primary interest.

Over the years, CLD optimisation of the shear dominated zone has been carried out in many different ways [2-11]. For a given damping material, the CLD system can be optimised in terms of location as well as the configuration of the treatments applied. The reliance of damping performance on treatment location and coverage area has been demonstrated numerically for beams [4, 19], frames [5] and plates [7, 20]. Most authors conclude that it is best to place the damping treatment on an area where the dynamic surface strain energy density (SED) of the host structure is highest (e.g., at a point of high modal curvature). As structures treated with CLD tend to be beam, plate or shell-like, their vibration properties in the lower frequencies are dominated by out-of-plane modes similar to bending and torsion modes in plates. For weight-efficient CLD applied to plates, the best configuration for the bending modes of a plate involves thin strips that run along the bending directions. For torsion-type modes, the optimum is a square patch whose edges are oriented with the principle stresses [17]. Assuming that the system is in the shear dominated zone, the desired size of these patches is controlled by the *shear* parameter – the relative shear stiffness of the damping layer (DL) normalised by the extensional stiffness of the constraining layer (CL) – as shown in Eqn. 1.

$$C = \frac{\text{shear stiffness of DL}}{\text{in - plane stiffness of CL}} = \frac{G_d L_c^2}{E_c t_c t_d} \tag{1}$$

where G is the shear modulus, E is the Young's modulus, L is the length, t is the thickness, and subscripts d and c refer to the damping and the constraining layers respectively.

In the literature, the shear parameter is expressed in a number of different ways as researchers have adapted its definition to suit the needs of their particular study. In order to avoid confusion, in this work, the parameter C in Eqn. 1 will be referred to as the *stiffness ratio*. For plates treated with different sized CLD patches, it has been shown that optimum damping of bending and torsion modes are achieved when C has a value of approximately 10 [17]. This agrees with the findings of Plunkett and Lee who considered CLD treatment attached to a beam under uniform strain [2]. An extension of Plunkett and Lee's work by Demoret and Torvik [21] showed that as the strain on the host becomes less uniform, the optimum stiffness ratio C increases.

3 Suitability of the Cellular Automata approach

Over the last thirty years, biological metaphors have proved invaluable in the design of powerful computational procedures for optimisation. Examples of these, well-used within engineering disciplines include the Genetic Algorithm, Differential Evolution and the Ant Colony Metaphor. These optimisers seek to maximise or minimise a given objective function. This paper, in studying Cellular Automata (CA), follows a slightly different approach that is not formally an optimisation procedure at all. Instead, the CA algorithms used here are designed to drive the solution towards desired performance criteria. The justification for this approach lies in the fact that there is a growing body of evidence that nature often aims to satisfy criteria rather than to optimise as this makes systems less fragile to uncertainty [22].

The cellular automaton achieves its performance objectives through the interactions between entities (individual cells of the 'organism') responsible for ensuring the appropriate performance of the system as a whole. The power and generality of the CA approach arise from the fact that a set of simple interacting processes with limited individual capability are able to construct arbitrarily complicated systems. In fact, it is known that particular CA schemes are Turing machines and thus universal computers [23].

Formally, a cellular automaton is a mathematical idealisation of a physical system in which space and time are discrete. In CA, the design domain is divided into a lattice of cells, each one capable of performing only one set of simple operations. Also, each cell may be in one of a finite number of states, S. These states are updated synchronously in discrete time steps, t, according to identical local rules $\mathcal{R}$, and these rules depend on the present states of the cell

and its neighbours within a certain proximity (neighbourhood) [24]. Eqn. 2 shows the evolution of the state of each cell at discrete position r, where $r + \Delta$ designates the cells belonging to a given neighbourhood of the CA.

$$S(r,t+1) = \Re[S(r,t), S(r+\Delta_1,t), ..., S(r+\Delta_N,t)] \quad (2)$$

The neighbourhood in CA, does not have any restrictions on size or location, except that it has to be the same throughout the entire lattice. The lattice structure however, is not limited to regular shape; an irregular shape of lattice is also possible. Fig. 1 shows commonly used CA neighbourhoods.

The selection of an appropriate performance measure is an important step in the construction of an effective algorithm that utilises CA. When constructing CA to design lightweight structures for carrying static loads, researchers have used the criterion of achieving uniform stress throughout the structure [13-15]. The hypothesis pursued in this paper is that for CLD location on a vibrating structure, satisfactory performance is achieved when the configuration of each segment of the treatment approaches an optimum shear stiffness (where the ratio of the modal loss factor to the loss factor of the VEM is maximised) for the given dynamic strain field.

4 Development and comparison of local rules for CLD design

4.1 Generic properties of CA rules used

Researchers applying CA to achieve uniform stress in statically loaded structures [13-15] produced algorithms that mimic a natural reorganisation process in bone, where the twin processes of cell birth and death (triggered by stress levels within the local neighbourhood) allow the structure to evolve. For the CLD evolution considered in this paper, the algorithms follow a growth principle rather than reorganisation. The exact approach used varies in each case and is described in detail in subsequent sections. In general however, the process involves seeding patches in suitable locations and growing them in the most productive directions until the performance (damping achieved for mass added) stops increasing.

As it is accepted that surface damping treatments work best in areas of high modal curvature, it is reasonable to locate the first cell of the added CLD at a point on the host structure where the modal SED is highest. While it is possible to define many rules that grow a CLD patch, not all will lead to efficient damping performance. One of the simplest approaches for growth

is to follow the SED profile of the host structure. This has been demonstrated for free-layer treatments in [16]. Another approach for CLD growth is to activate cells that dissipate most energy. The challenge with CLD is that elements that individually dissipate most energy are not necessarily the most important when it comes to optimising the whole patch. Often, cells near the centre of a patch dissipate very little energy but do provide stiffness for the CL – a crucial factor affecting performance, according to Eqn. 1. For this reason, local rules have to account for the performance of each patch as a whole.

Conventional CA rules update all cells in the design domain at discrete "time" steps. In this study, a "time" step refers to one analysis stage and involves at least one FE calculation, in which the damping performance of individual elements (and hence the system) is calculated. To avoid overlapping, a patch-by-patch growth strategy is followed. The local neighbourhood in which growth can occur is defined by the entire patch rather than by individual cells acting independently. For example, Fig. 1 shows two types of neighbourhood for a patch comprising two cells. Four different CA algorithms for selecting elements within a neighbourhood are considered. Their effectiveness is assessed by evaluating their ability to achieve known optimal configurations.

4.2 Modelling approach

For the CLD location studies described here, it was considered desirable to restrict FE calculations to eigenvalue extraction rather than forced response to avoid excessive computational cost. To allow direct comparison between patches of different size, the effectiveness of a particular CLD treatment was quantified as the loss factor ratio per unit added mass. The Modal Strain Energy (MSE) approach [25] gives

$$\text{Loss factor ratio} = \frac{\eta}{\eta_v} = \frac{U_d}{U_{total}} \tag{3}$$

where η is the modal loss factor, U_d is the modal strain energy in the viscoelastic material (or damping layer, DL) and U_{total} is the total strain energy for that mode.

While it is well-known that the MSE approach can provide inaccurate results for systems with high VEM loss factors (η_v) or with strongly frequency dependent properties, it was considered appropriate for this study because the focus of the study is to compare relative merits of a CA algorithm for optimising CLD treatments. Higher fidelity analyses such as direct forced response, complex eigenvalues or the modified MSE (MMSE) approach [26] would add

complexity without necessarily increasing understanding as optimum patch geometry is only weakly affected by frequency dependence and VEM loss factor. Instead, in the work presented here, the elastic modulus values are assumed constant over all frequencies and the loss factor of the VEM, η_v is set as 0.3. For these properties, the MSE approach is accurate [27]. Note however, that the approach used is equally compatible with the higher-accuracy prediction procedures.

In the studies reported here, the host structure and CLD treatment were modelled using the commercial software package Abaqus. The DL was modelled using 20 noded, solid brick elements. The host structure and the CL were represented using 8 noded shells. The shell elements used an offset formulation that allowed their definition using the same face nodes as the brick elements. This ensured displacement and strain compatibility between the layers. In the studies presented here, the grid of CA cells was aligned to the FE mesh and each cell was one element in size (10 mm square elements were used in most cases). Activation of a cell involved placing one solid (DL) and one shell (CL) element onto an existing element on the host structure. In practice, larger cells comprising several elements could also be used. The benefit would be a reduction in iterations required to achieve a given coverage at the cost of reduced spatial resolution.

4.3 Optimum CLD configuration for the first torsion and bending modes

In order to assess the effectiveness of each algorithm used, their performance was tested on a system for which the optimum configuration for CLD is known. Here, the effectiveness of each proposed CA local rule in dealing with the two vibration modes (torsion and bending) of a rectangular plate with free boundaries [17] was assessed by evaluating their ability to achieve known optimal configurations. The dimensions and properties for the host structure and the CLD treatment are shown in Table 1.

Fig. 2 shows the normalised in-plane direct and shear strains of the host structure for Mode 1, the first torsion mode. It can be seen that the centre of the plate is subjected primarily to in-plane shear strain while edges experience direct strains associated with local out-of-plane bending. Also, the shear strain levels are around five times higher than those for direct strains. As the principal stress/strain axes in the shear dominated zone are oriented at 45° to the plate edges, the optimum configuration for the CLD treatment at the centre for this mode should resemble a diamond shape [17]. To be optimum however, the effective length should be such that the stiffness ratio C, is approximately 10. This gives the optimum CLD patch for the

torsion mode as a centrally located square with sides approximately 130mm in length, whose diagonals lie parallel to the edges of the plate.

Fig. 3 shows the contour plot of the SED for Mode 2, the first bending mode along the length-direction. For this type of mode, thin strips of treatment along the bending direction are most efficient for a given added mass [17]. To be optimum however, the length for the CLD treatment should be, according to Eqn. 1, approximately 130mm. In this study, damping effectiveness obtained, together with its computational time required with different CA rules are summarised in Table 2.

4.4 Algorithm CA-1

Inspired by earlier work on free-layer systems [16], one approach for CLD growth is to follow the SED profile of the host structure; i.e., to grow where the SED is maximum. The elements in which growth can occur are defined by the Moore neighbourhood of the active patch. To monitor patch evolution and for comparison with other approaches, the algorithm limits the CLD growth to a single cell per FE analysis iteration.

Once a patch ceases to grow, because the addition of treatment ceases to give an improvement in damping effectiveness, a 'stay-out' zone of a Moore neighbourhood is activated around this patch in order to avoid overlapping of subsequent patches. The reason for this stay-out zone is to maintain the damping performance of the completed patch. This only really occurs if the deformation field around the optimised patch does not change on addition of new patches. While it is reasonable to assume that for most treatments, mode shapes do not change dramatically through the addition of CLD, this assumption may become a source of error when particularly thick or heavy constraining layers are studied. In this paper, this algorithm is called CA-1 and its principal steps are summarised below.

1. The algorithm starts by adding a single CLD patch to the plate FE mesh at the point of highest modal SED.
2. The cell with highest host structure SED within the Moore neighbourhood of the activated CLD patch is selected for the next iteration.
3. The growth of a particular patch is terminated when addition of CLD treatment ceases to give an improvement in damping effectiveness.
4. A stay-out zone, defined by the Moore neighbourhood, is activated around the completed patch.

5. A new patch is generated by repeating Steps 1 – 4.

The stopping point for all the CA rules discussed in this paper can be selected by the user – as a preset number of treatment patches, a desired overall treatment coverage or a predefined damping level. With CA-1, Fig. 4 and 5 show the evolution of the damping treatment obtained at 2%, 6% and 10% coverage, for Modes 1 (torsion) and 2 (bending) respectively. Results obtained show that CA-1 is not suitable for optimising the torsion mode, as the resulting shape of the damping treatment is different from the expected optimum shape (a square patch oriented at 45°). While CA-1 manages to produce some thin strips of treatment for the bending mode, their length at 50mm is much less than the optimum value of 130mm. From these results, it is clear that CA-1 is not suitable for CLD design. Since the algorithm locates a new CLD cell based on the information from a single (most updated) FE analysis, the algorithm progresses rapidly: coverage of 10% was achieved with less than 150 FE evaluations.

4.5 Algorithm CA-2

Since the objective is to improve the damping performance of the CLD system, another possible approach for CLD growth is to activate cells that benefit the existing patch the most. This is achieved by comparing the performance of a number of patches, each patch comprising the original cells plus one from the Moore neighbourhood around the patch. The new patch with the highest damping is then selected. In this way, this algorithm includes a "survival-of-the-fittest" mechanism, albeit only in the outermost layer of elements. This rule is called CA-2 in this paper. The principle steps in CA-2 are summarised below.

1. The algorithm starts by adding a single CLD patch to the plate FE mesh at the point of highest modal SED
2. The damping effectiveness (loss factor ratio per added mass) is calculated for as many patches as there are cells in the Moore neighbourhood, each comprising the original cells plus one from the neighbourhood.
3. The patch with the highest damping effectiveness is selected for the next iteration.
4. The growth of a particular patch is terminated when addition of CLD treatment ceases to give an improvement in damping effectiveness
5. A stay-out zone, defined by the Moore neighbourhood, is activated around the completed patch.

6. A new patch is generated by repeating Steps 1 – 5.

Fig. 6 and 7 show the evolution of the damping treatment obtained at 2%, 6% and 10% coverage from CA-2, for Modes 1 and 2 respectively. As a number of possible choices of new patches are pre-evaluated at each evolution step, this approach requires approximately 10 times the number of FE evaluations than CA-1. From the results, it is clear that CA-2 is able to optimise the bending mode as it produces thin strips of treatment at the optimum length of 130mm. Though the resulting treatment coverage for the torsion mode is not optimum, CA-2 manages to produce regular strips of coverage oriented at 45° to the plate edges. However, as the strips are at 45° to the grid and only one element wide, their physical interpretation is uncertain – particularly at the connecting nodes (see Fig. 6). To maintain a measurable width over the length of the strip, CA-2 was modified such that it activates an extra neighbouring cell.

With this modified CA-2, the resulting treatment configuration for the first bending mode is identical to the one obtained from CA-2, while Fig. 8 shows the evolution of the damping treatment obtained at 2%, 6% and 10% coverage for the first torsion mode. It is important to note that the lengths of these thin strips are on average approximately 110mm; closer to the expected optimum length compared to those obtained from CA-2 (100mm). Thus while modified CA-2 is not perfect, it is a significant improvement on CA-1.

4.6 Algorithm CA-3

Results from modified CA-2 show that activating a single cell of CLD treatment per iteration can trap the process in local optima: a thin strip does not thicken because the addition of a single cell to the side of a strip already at optimum length (but not optimum width), creates a segment of the patch with suboptimal shape – improved performance is only achieved when all the cells along the side are added. In order to avoid this trap, CA-3 grows the CLD treatment by activating strips of cells rather than single cells per FE iteration – the main points are summarised below.

1. The algorithm starts by adding a single CLD patch to the plate FE mesh at the point of highest modal SED
2. The damping effectiveness is calculated for four different patches – each comprising the original cell plus one side of the von Neumann neighbourhood.
3. The patch with the highest damping effectiveness is selected for the next iteration.

4. The growth of a particular patch is terminated when addition of CLD treatment ceases to give an improvement in damping effectiveness
5. A stay-out zone, defined by the Moore neighbourhood, is activated around the completed patch.
6. A new patch is generated by repeating Steps 1 – 5.

With CA-3, the resulting treatment for the first bending mode is exactly the same as the one obtained from CA-2, while Fig. 9 shows the evolution of the damping treatment obtained at 2%, 6% and 10% coverage for the first torsion mode. Unlike previous CA rules, the growth of the CLD treatment in CA-3 is constrained within a von Neumann neighbourhood. An advantage of using the von Neumann neighbourhood is that it halves the number of possible new patch locations compared to a Moore neighbourhood. Additionally as this algorithm adds elements as strips, coverage is built up more quickly. To achieve 10% coverage, typically 450 FE analyses were needed for the bending modes and only 150 for the torsion mode (as it requires fewer patches). However, the consequence of this is that it can only produce rectangular patches with edges parallel to the plate edges. Nevertheless, damping effectiveness obtained at 10% coverage (as recorded in Table 2) shows that CA-3 outperforms both CA-1 and CA-2. Close observation also shows that the diagonal length of the CLD treatment is approximately 130mm – the expected optimum.

4.7 Algorithm CA-4

To allow growth of the patch at an angle to the grid, a final algorithm, CA-4 was defined. This combined the idea of activating strips of cells (CA-3) with ability to create diagonal strips (CA-2). In CA-4, the initial stages are similar to CA-2, as cells are added one by one. However, once the addition of single cells ceases to give an improvement in damping effectiveness, the patch is able to add strips of cells per FE iteration. In order to allow more flexibility in the CLD growth, the Moore neighbourhood is used for growing the strips of cells. The key steps in the algorithm are described below.

1. The algorithm starts by adding a single CLD patch to the plate FE mesh at the point of highest modal SED
2. The damping effectiveness is calculated for as many patches as there are cells in the Moore neighbourhood. The patches comprise the original cells plus one from the neighbourhood if the added cell shares at least one edge with the original ones. If the

extra cell only shares a node with the original patch, an adjacent cell from the neighbourhood is also activated.

3. The patch with the highest damping effectiveness is retained.
4. The growth of the CLD patch changes from a single cell to strips of cells once the addition of single cells ceases to give an improvement in damping effectiveness.
5. The damping effectiveness is calculated for twelve different patches – each comprising the original cells plus one possible adjacent strip of cells within the Moore neighbourhood (see Fig. 10).
6. The patch with the highest damping effectiveness is selected for the next iteration. The patch illustrated in Fig. 10(n) assumes patch (f) gives the highest damping effectiveness.
7. The growth of a particular patch is terminated when the addition of strips ceases to give an improvement in damping effectiveness
8. A stay-out zone, defined by the Moore neighbourhood, is activated around the completed patch.
9. A new patch is generated by repeating Steps 1 – 8.

The resulting treatment configuration obtained for the first bending mode is exactly the same as the one obtained from CA-2 and CA-3, while Fig. 11 shows the evolution of the damping treatment obtained at 2%, 6% and 10% coverage for the first torsion mode. As this approach uses the Moore neighbourhood for identifying possible patch locations, it requires a greater number of FE analyses. To achieve a coverage of 10%, approximately 1500 FE analysis calculations were required. Results obtained show that the patch at last achieves the known optimal shape for the torsion mode. Table 2 shows that the damping effectiveness obtained from CA-4 is the best among the developed CA rules. Besides, the dimensions of CLD patches generated correspond well with the analytical work for optimum CLD length in [2] and [17]. Hence, it is clear that CA-4 is capable of finding the appropriate CLD coverage for both torsion and bending modes. Note that the highest damping effectiveness obtained for the first torsion mode (close to 0.88) is less than that for the first bending mode (close to 1.35). The reason for this is that in the bending mode, the strain energy of the host structure is concentrated to a greater extent in the zone where the CLD treatment is applied: the fraction of energy in the treated zone is about 0.144 in the torsion mode and 0.210 in bending. In each

case therefore, the configuration induces in the viscoelastic layer approximately 9% of the energy that is found in the host structure that is directly below it.

Using CA-4, it can be seen therefore, that suitable damping treatments can be created relatively quickly. While the number of FE analysis runs required depends directly on the coverage area (as the treatment is "grown" over the surface), desirable configurations were generally achieved within a few hundreds of FE calculations. This implies significantly reduced computational cost in comparison to optimisation routines such as the Downhill Simplex or Genetic Algorithm.

5 CA algorithm applied to several modes of a curved composite panel

Work presented in the previous section showed that CA-4 is suitable for creating CLD treatments for single vibration modes. However, in real-life applications, vibrations often occur over a wide frequency range, where a number of resonances may get excited. This section considers the design of a CLD system for a number of vibration modes simultaneously using CA-4. For this study, a cylindrically curved (2m radius) composite panel was used. The panel was made from carbon fibre and its nominal properties are shown in Table 3. In order to reduce the computational cost, the cell and FE mesh size was increased to 20 by 20mm. In this case, 20 noded, solid brick elements were used to model the host structure and the damping layer while offset shell elements were used for the CL as before.

For the panel, the first four resonances occur below 100Hz; where Modes 1, 3 and 4 are torsion-type modes and Mode 2 involves bending along the direction of curvature. To obtain a single "fitness" function for assessing performance, a weighting parameter is applied to each mode of interest; with the sum of the weighting parameters equal to unity. The objective of the evolution was then to maximise the "fitness", i.e. the sum of the weighted damping effectiveness levels. In this paper, two formats for the weighting parameter were considered:

1. Equal weighting parameter for each mode.
2. Unity weighting parameter for the weakest mode, zero for the others.

The first approach is equivalent to averaging the damping effectiveness over each mode of interest. Since the algorithm focuses on activating CLD cells that give a highest possible fitness, the dominant mode (vibration mode with the highest modal loss factor) will have the greatest effect on the evolution. The second approach however, focuses on improving the

weakest mode (vibration mode with the lowest modal loss factor). Hence, the algorithm activates CLD cells that give a highest possible modal loss factor on the weakest mode. Here, the initial condition for both the algorithms was made similar where the first cell of CLD was located at the maximum averaged SED zone.

The dimensions and the material properties of the host structure and the CLD treatments are shown in Table 3 and Fig. 12. As this study was carried out with practical implementation in mind (see Section 6), a real damping material was used in the optimisation. Here, the well-known CLD material, ISD 112 was used for the DL while the CL was made from thin shim steel. Note that the shear modulus and the material loss factor of ISD112 change with frequency and the temperature (see Fig. 12). The algorithm CA-4 was run assuming a single averaged value for the VEM shear modulus G_d which was obtained assuming a temperature of 21°C and frequencies of 19.0, 60.5, 71.4, 96.1 Hz relating to the natural frequencies of the untreated panel. Damping predictions were carried out using the MSE method as before.

Fig. 13 shows the first two patches generated by the algorithm CA-4 for the curved composite panel with a uniform weighting parameter (i.e. 0.25) over the first four modes. The total coverage for these patches is 13.1% and they are trapezoidal in shape. With this CLD configuration, the highest modal loss factor obtained is 4.4% for Mode 3 while the lowest is 0.1% for Mode 4, as shown in Table 4. For a particular patch, the optimality with regard to size relates approximately to the stiffness ratio C. According to Eqn. 1, for $C \approx 10$ the optimum characteristic length is between 220 and 330mm, for the first four modes. It can be seen that the patches generated are around this size. However, as the strain distribution is more complicated than on the plates considered earlier, it is not possible to identify a single direction in which to measure the characteristic length. An alternative way to estimate the optimality of a particular configuration is to monitor the damping performance whilst altering C. Here, this was achieved by altering the VEM shear modulus G_d – results are presented in Fig. 14. It can be seen that while the first 3 modes are indeed near their optimum, the fourth mode is not even close. Thus it can be seen that a uniform weighting parameter skews results in favour of modes with the highest damping.

The alternative strategy considered – focusing effort on the weakest mode – produced the configuration shown in Fig. 15. It is interesting to note that the locations for the new optimised patches are completely different from those obtained with the uniform weighting parameter. The optimality plot (Fig. 16), shows that all four modes are relatively close to their optimum. Note that the patches applied here are somewhat larger than those seen previously:

the total coverage is 22.2% (with uniform weighting parameter this was 13.1%) which explains the increase in modal loss factors seen in Table 4.

Note that on a symmetrical structure such as this, one would expect the optimised treatment to be symmetrical. While the result obtained using the uniform weighting parameter (Fig. 13) corresponds quite well to this, the two patches obtained using the "weakest mode" weighting parameter (Fig. 15) is far from symmetrical. In an attempt to understand this, the surface strain on the panel was studied as damping patches were added. Plots showing the surface SED for the weakest mode (Mode 4) are presented in Fig. 17. The plots relate to the plate with no CLD and with one and two optimised patches obtained from the "weakest mode" weighting parameter respectively. These figures show that the strain distribution on the host structure changes somewhat as the first patch is added and symmetry is lost.

While the resulting CLD configurations are encouraging in terms of performance, their unusual shapes are not convenient for fabrication. The shapes were therefore manually smoothed by trimming off protrusions and filling voids. Fig. 18 and 19 show the resulting shapes based on Fig. 13 and 15 respectively. Minimal changes in damping performance are caused by smoothing, as can be seen in Table 4. This indicates that the evolved configuration is relatively insensitive to uncertainty.

The fact that the combined area of the two smoothed patches generated using a uniform weighting parameter (see Fig. 18) is approximately equal to the area of the first smoothed patch generated using the "weakest mode" weighting parameter (see Fig. 20), allows a back-to-back comparison of performance to be made. In ensuring that the fourth mode is damped, the second method significantly reduces the effectiveness of Modes 2 and 3 (refer to Table 4). Thus it can be seen that the correct definition of the fitness function is essential for getting a suitable CLD configuration. While a detailed discussion of suitable fitness or cost functions for optimisation is beyond the scope of this paper, it is clear that it is advisable to limit the optimisation to modes that really do need damping.

6 Experimental validation of the optimised CLD treatment

As a number of simplifications were made in the analyses described in Sections 4 and 5, predicted natural frequencies and damping levels for one condition were validated experimentally.

The curved composite panel (described in Section 5) was first tested without any damping treatment. To approximate free boundary conditions, the curved panel was suspended on soft springs. A photograph showing the suspended panel, including small clamps, nylon line and coil springs used to approximate the free (no stiffness, no damping) boundaries is presented in Fig. 21. The structure was excited at 25 different points using a PCB type 086C03 instrumented hammer and the response measured using a PCB type M353B16 accelerometer positioned at one corner of the panel. Data acquisition was controlled using a LMS test system running Modal Impact Test software. The sampling frequency was set at 256 Hz in order to capture the force pulse accurately. The acquisition time was set to get a frequency resolution of 0.125 Hz. At each point, 10 averages were taken.

The built-in PolyMax algorithm was used to estimate modal properties from the test data. The close match between predicted and measured mode shapes for the first four modes of the untreated panel are presented in Fig. 22. A comparison of predicted and measured natural frequencies is given in Fig. 23. Together these results show that the model for the untreated panel represented the dynamics of the actual system accurately. Note that as part of its parameter estimation procedure, LMS software generates a stabilisation diagram from the test results. This allows the user to select a number of "stabilised" modes to represent the system. The variation in the stabilised modes offered at each resonance is a measure of the uncertainty in the parameter estimation process and differences in individual responses measured during the test. Each of these points is represented as a dot in Fig. 23. The experimental work also showed that some damping existed in the experimental set-up. This was assumed to come from the supports, the composite material and the transducer cabling. The average value for each mode was taken to be the background damping for that mode.

A patch of CLD material, identical to the first optimised patch (smoothed) obtained using the "weakest mode" weighting, was cut to size and fixed in place on the panel as shown in Fig. 21. As the aim was to validate the model, the shape was cut to match the FE grid. In a practical application the patch would be simplified further by replacing the zig-zag cuts by straight lines. The measurement described above was repeated. As temperature affects properties of ISD112 significantly, a thermocouple was used to measure surface temperature before the test. This was found to be 23°C. As this was slightly warmer than the originally assumed value, the prediction was re-run to accommodate this change.

A comparison of measured and predicted natural frequency and damping levels for the system are presented in Fig. 24. Note that measured damping values shown in Fig. 24 represent the

added damping. This was estimated by subtracting the background damping (from the untreated panel) from the measured modal damping value. Predicted values were estimated in two ways. In the first (represented in Fig. 24 by a circle), an improved version of the Modal Strain Energy approach (denoted MMSE) [26] was used with material data taken at 23°C, as MMSE analysis has been shown to give more accurate (slightly underestimated) damping predictions for viscoelastic systems with high loss factor (>0.3) [27]. The MMSE approach gives

$$\text{Loss factor ratio} = \frac{\eta}{\eta_v} = \frac{\overline{R}}{\alpha + (1-\alpha)\overline{R}} \tag{4}$$

$$\text{where} \quad \alpha = \sqrt{1+\eta_v^2} \quad \text{and} \quad \overline{R} = \frac{\overline{U}_d}{\overline{U}_{total}}$$

where η is the modal loss factor, η_v is the VEM loss factor, $\overline{U}_d$ and $\overline{U}_{total}$ are the modal strain energy in the DL and the total strain energy for that mode obtained using the magnitude of the complex modulus; i.e., $\overline{E} = E\sqrt{1+\eta_v^2}$.

In the second prediction, efforts were made to account for the uncertainties in the calculation. As the MSE and MMSE methods provide upper and lower bounds respectively for the damping [28], both approaches were used. Also, since the experiment lasted for approximately 3 hours, the temperature of the VEM was assumed to vary from 22 to 24°C. The extreme points obtained in this way were used to define a box within which predicted results would be expected to lie. Fig. 24 shows that the damping measurements lie within the estimates and are close to the predicted single-point value. In general the predicted frequencies are also relatively close.

More generally, one might comment on the fact that optimised damping levels achieved are relatively low – only 1 to 3 % for the single patch tested. The reason for this is because the constraining layer available for this study was relatively thin. Taking this into account, the damping achieved is significant – the total mass of the added layer was only 73 grams, less than 4% of the mass of the host structure made of carbon fibre composite.

From this work, it can be concluded that the FE predictions for the resonance frequency and the modal loss factor are acceptable and they show that the FE approach used has adequate accuracy.

7 Conclusions

This paper has demonstrated the use of CA local rules for CLD design. Four CA rules were developed to grow CLD treatments on structures. The performance of each of these algorithms was assessed for bending and torsion modes on a flat aluminium plate using the known optimal CLD configurations. The presented work showed that the best CA rule developed (CA-4) can optimise CLD effectively. The next best rule (CA-3) was equally effective for bending modes but was around 20% less effective at dealing with modes with significant in-plane shear. However, as it requires less than a third of the computational effort, it may be the best choice in some circumstances.

CA-4 was then used to optimise the CLD on a curved composite panel for the first four modes. For multi-mode optimisation, results obtained show that different settings in the weighting parameter dramatically affected the final solution. Experimental verification on the optimised CLD curved panel showed that overall FE predictions of both the resonance frequency and its modal loss factor are acceptable.

The best CA rule developed has shown to be well suited to problems where the CLD treatment is relatively thin in comparison to the host structure. In this paper, the CA approach has been demonstrated on a plate and an orthotropic shell. However, the method is equally applicable for any suitable structure provided that a reasonably accurate FE model can be created. In practice, CLD is applied to a wide range of structures including aircraft panels with stringers and stiffeners, vehicle engine covers and brake pad insulators [29]. Where the host structure mesh is based on quadratic elements, the algorithm CA-4 could be used directly. For meshes based on triangular shape, some modifications may be necessary.

More generally, the paper has demonstrated the importance of the exact rule base that the CA procedure uses. In this case, local rules that account best for CLD optimisation criteria perform the most successfully.

Acknowledgement

The authors would like to thank Rolls-Royce plc for their support of this work. The views expressed in this paper are those of the authors and are not necessarily those of Rolls-Royce plc.

References

1. D J Mead, *Passive Vibration Control, Wiley*, 1998.
2. R Plunkett and C T Lee, Length optimization of constrained viscoelastic layer damping, *The Journal of the Acoustic Society of America,* 48 (1), 150-161, 1970.
3. D K Rao, Frequency and loss factors of sandwich beams under various boundary conditions, *IMechE Journal of Mechanical Engineering Science,* 20 (5), 271-282, 1978.
4. R Lunden, Optimum distribution of additive damping for vibrating beams, *Journal of Sound and Vibration,* 66 (1), 25-37, 1979.
5. R Lunden, Optimum distribution of additive damping for vibrating frames, *Journal of Sound and Vibration,* 72 (3), 391-402, 1980.
6. J M Lifshitz and M Leibowitz, Optimal sandwich beam design for maximum viscoelastic damping, *International Journal of Solids and Structures,* 23 (7), 1027-1034, 1987.
7. Y C Chen and S C Huang, An optimal placement of CLD treatment for vibration suppression of plates, *International Journal of Mechanical Sciences,* 44, 1801-1821, 2002.
8. P Hajela and C Y Lin, Optimal design of viscoelastically damped beam structures, *Applied Mechanics Reviews,* 44 (11 Part 2), S96-S106, 1991.
9. M A Trindade, Optimization of sandwich/multilayer viscoelastic composite structure for vibration damping. *Proceedings of OMAE'01, 20th International Conference on Offshore Mechanics and Arctic Engineering,* Brazil, 2001.
10. H Zheng, C Cai, and X M Tan, Optimization of partial constrained layer damping treatment for vibrational energy minimization of vibrating beams, *Computers and Structures,* 82, 2493-2507, 2004.
11. M Alvelid M, Optimal position and shape of applied damping material, In Press, *Journal of Sound and Vibration*.
12. A Wuensche A and M Lesser, *The Global Dynamics of Cellular Automata.* Addison-Wesley Publishing Company, Wokingham, England, 1992.
13. N Inou, N Shimotai, and T Uesugi, A cellular automaton generating topological structures. *2nd European Conference on Smart Structures and Materials,* Glasgow, 1994.

14. K Worden, and G R Tomlinson, On structures from cellular automata. Proceedings of International Symposium on Microsystems, Intelligent Materials and Robots, Sendai, Japan, 1995.

15. A Tovar, N Patel, A K Kaushik, G A Letona and J E Renaud, Hybrid Cellular Automata: a biologically-inspired structural optimization technique, *10th AIAA/ISSMO Multidisciplinary Analysis and Optimization Conference,* New York, 2004.

16. R Wardle and G R Tomlinson, Structural design for dynamic loading using biomimetic approach. *Proceedings of SPIE, Smart Structures and Materials 1997: Smart Materials Technologies*, 1997.

17. C M Chia, J A Rongong and K Worden, Evolution of constrained layer damping using a Cellular Automaton algorithm, In press, *IMechE, Part C, Journal of Mechanical Engineering Science*.

18. J A Rongong and G R Tomlinson, Suppression of ring vibration modes of high nodal diameter using constrained layer damping methods, *Smart Materials and Structures,* 5, 672-684, 1996.

19. P R Mantena, R F Gibson and S J Hwang, Optimal constrained viscoelastic tape lengths for maximizing damping in laminated composites, *AIAA Journal,* 29 (10), 1678-1685, 1991.

20. A K Lall, N T Asnani and B C Nakra, Vibration and damping analysis of rectangular plate with partially covered constrained viscoelastic layer, *Journal of Vibration, Acoustics, Stress, and Reliability in Design,* 109, 241-247, 1987.

21. K J Demoret and P J Torvik, Optimal length of constrained layers on a substrate with linearly varying strain, *Proceeding of the ASME Design Engineering Technical Conference,* 3(c), 719-726, 1995.

22. Y Ben-Haim, *Info-Gap Decision Theory : Decisions under Severe Uncertainty, 2nd edition, Academic Press*, 2006.

23. S Wolfram, *A New Kind of Science.* Wolfram Media, Canada, 2002.

24. P P Chaudhuri, D R Chowdhury, S Nandi, and S Chattopadhay, *Additive Cellular Automata: Theory and Application.* IEEE Computer Society Press, California, 1997.

25. C D Johnson and D A Keinholz, Finite element prediction of damping in structures with constrained viscoelastic layers, *AIAA Journal,* 20 (9), 1284 – 1290, 1982.

26. J A Rongong, Reducing vibration levels using 'Smart Joint' concepts, *Proceedings of ISMA 25, Noise and Vibration Engineering Conference,* Leuven, 817-824, 2000.

27. F Scarpa, F P Landi, J A Rongong and G R Tomlinson, Improving the MSE method for damped structures using a dyadic matrix perturbation approach. *Proceedings of the IMechE Part C: Journal of Mechanical Engineering Science*, 216, 1207-1216, 2002.

28. J A Rongong, Shear and extensional behaviour of passive and active constrained layer damping, PhD thesis, The University of Sheffield, 2002.

29. M D Rao, Recent applications of viscoelastic damping for noise control in automobiles and commercial airplanes, *Journal of Sound and Vibration,* 262 (3), 457 – 474, 2003.

Figure Captions

Figure 1: Commonly used neighbourhoods – hatched areas show (a) the Von Neumann neighbourhood and (b) the Moore neighbourhood of the black element.

Figure 2: Contour plot of normalised (a) in-plane shear strain, and direct strain in the (b) length and (c) width direction for Mode 1

Figure 3: Contour plot of the SED on the host structure for Mode 2 (heavy shading indicates high SED)

Figure 4: (a) 2% (b) 6% and (c) 10% treatment coverage for Mode 1 (first torsion mode), obtained using CA-1

Figure 5: (a) 2% (b) 6% and (c) 10% treatment coverage for Mode 2 (first bending mode), obtained using CA-1

Figure 6: (a) 2% (b) 6% and (c) 10% treatment coverage for Mode 1 (first torsion mode), obtained using CA-2

Figure 7: (a) 2% (b) 6% and (c) 10% treatment coverage for Mode 2 (first bending mode), obtained using CA-2

Figure 22: Mode shapes for first four modes of the untreated panel

Figure 23: Plot showing the FE predictions (line) on the resonance frequency and the experimental measurements (dot) on both the resonance frequency and its modal loss factor, for untreated curved panel

Figure 24: Plot showing the resonance frequency and its modal loss factor measured by LMS system (dot); predicted by MMSE (circle)using the average VEM Young's modulus at 23°C; upper and lower bound (square) predicted using both the MSE and MMSE method with temperature varying from 22–24°C

Figures

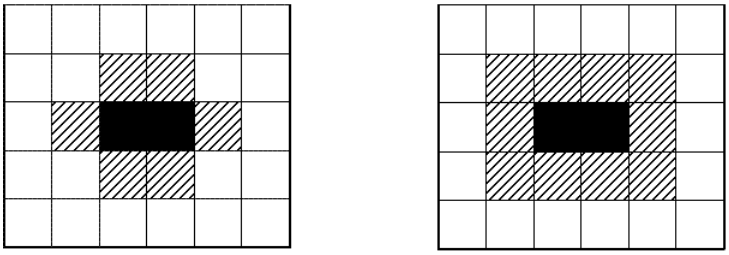

(a) (b)

Figure 1: Commonly used neighbourhoods – hatched areas show (a) the Von Neumann neighbourhood and (b) the Moore neighbourhood of the black element.

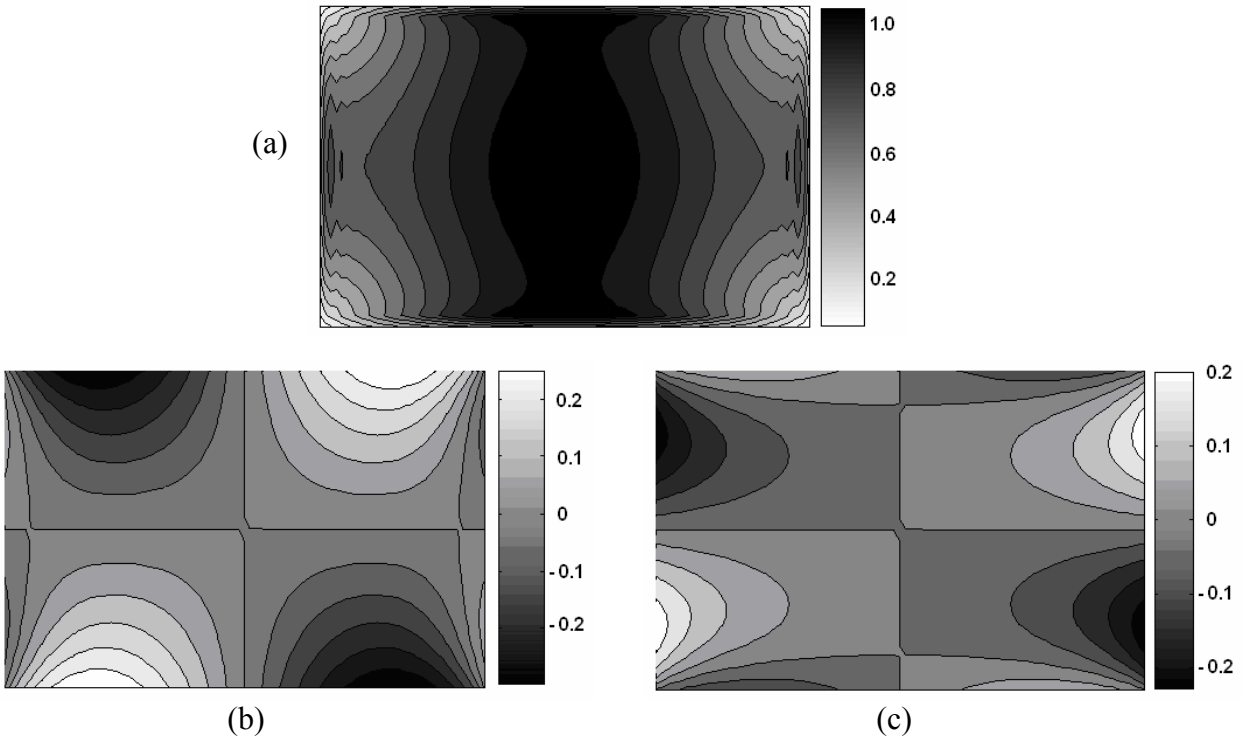

Figure 2: Contour plot of normalised (a) in-plane shear strain, and direct strain in the (b) length and (c) width direction for Mode 1

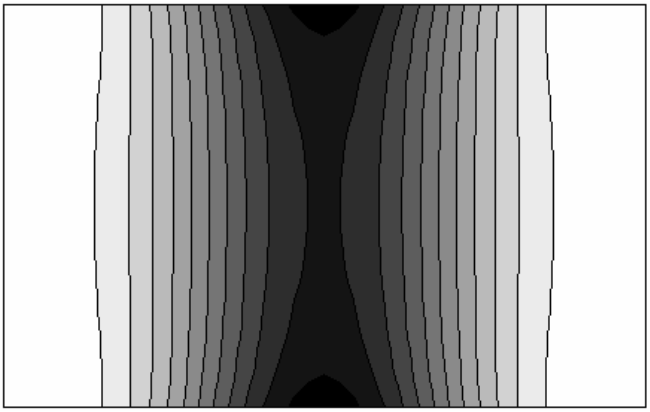

Figure 3: Contour plot of the SED on the host structure for Mode 2 (heavy shading indicates high SED)

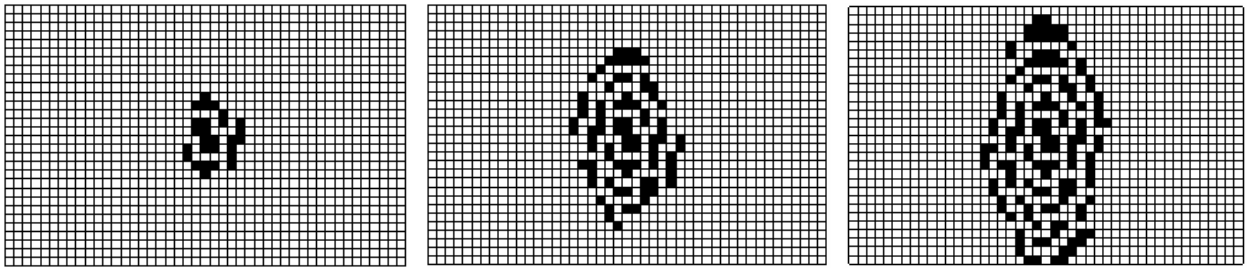

Figure 4: (a) 2% (b) 6% and (c) 10% treatment coverage for Mode 1 (first torsion mode), obtained using CA-1

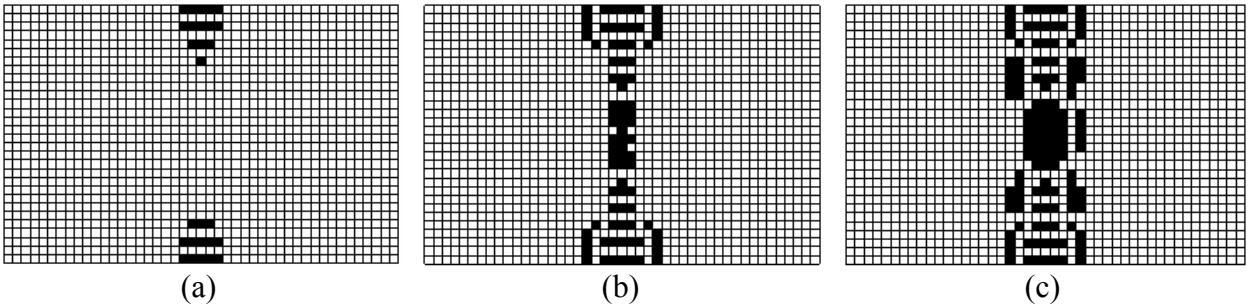

Figure 5: (a) 2% (b) 6% and (c) 10% treatment coverage for Mode 2 (first bending mode), obtained using CA-1

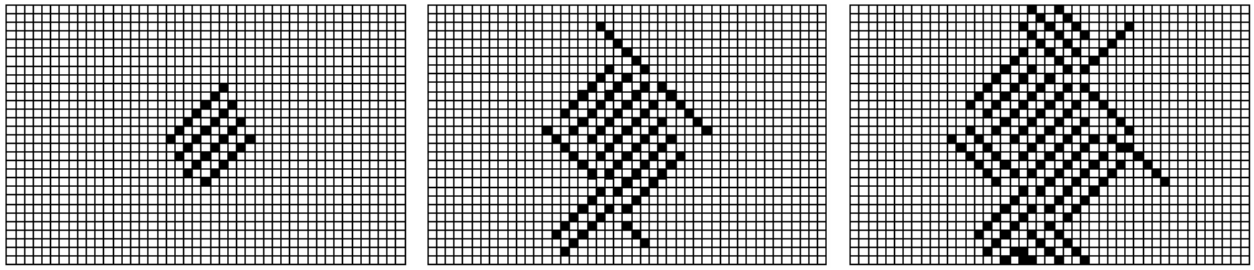

(a) (b) (c)

Figure 6: (a) 2% (b) 6% and (c) 10% treatment coverage for Mode 1 (first torsion mode), obtained using CA-2

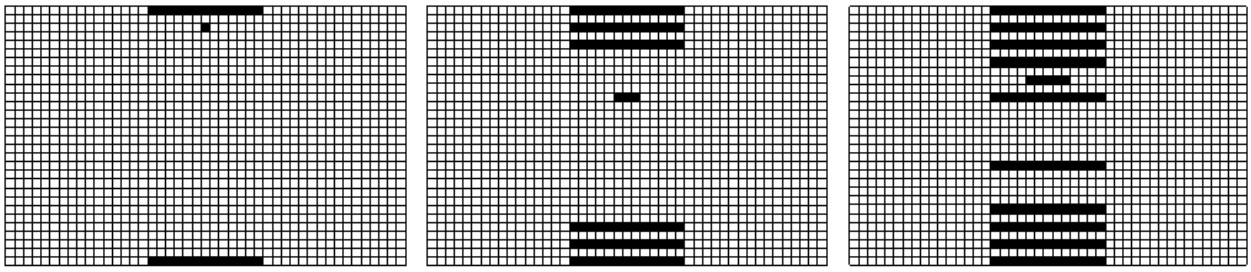

(a) (b) (c)

Figure 7: (a) 2% (b) 6% and (c) 10% treatment coverage for Mode 2 (first bending mode), obtained using CA-2

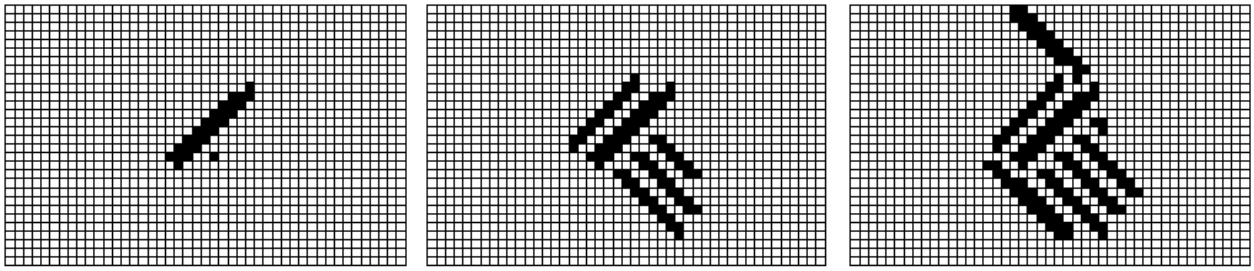

(a) (b) (c)

Figure 8: (a) 2% (b) 6% and (c) 10% treatment coverage for Mode 1 (first torsion mode), obtained using modified CA-2

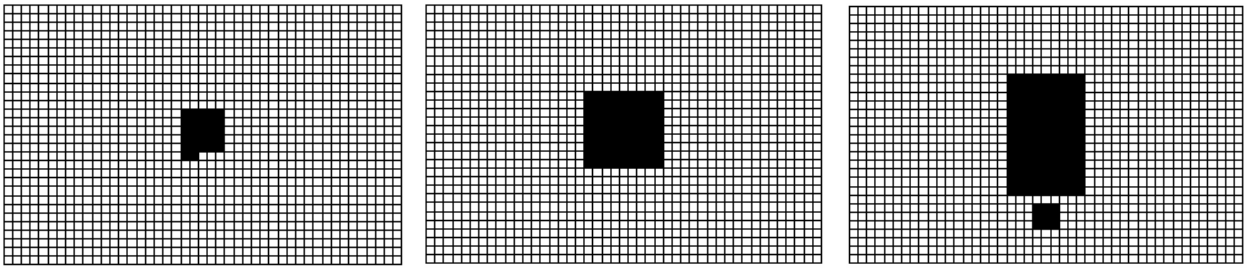

Figure 9: (a) 2% (b) 6% and (c) 10% treatment coverage for Mode 1 (first torsion mode), obtained using CA-3

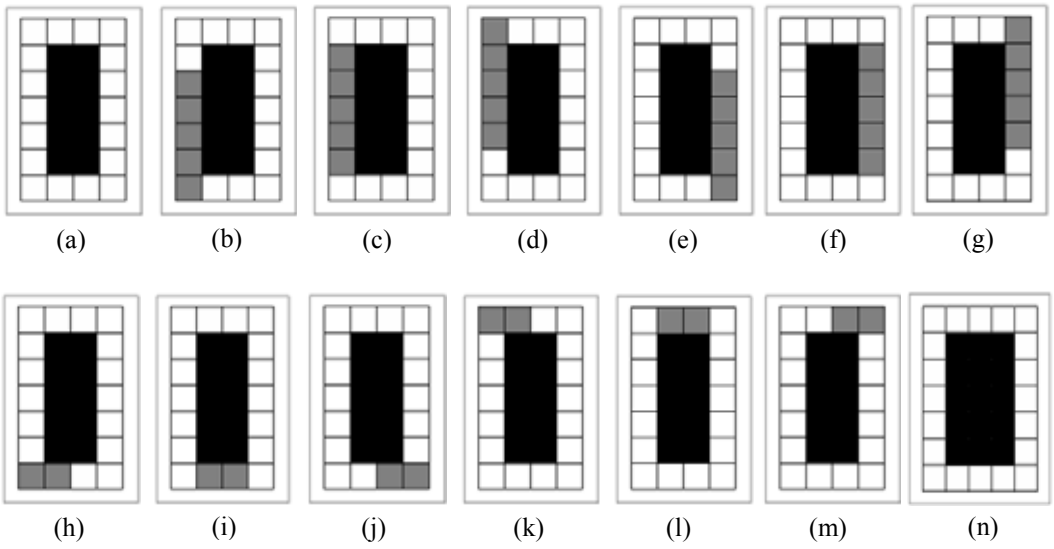

Figure 10: Steps involved in patch growth a) initial patch and neighbourhood, b) to m) different patches analysed, n) new patch and neighbourhood

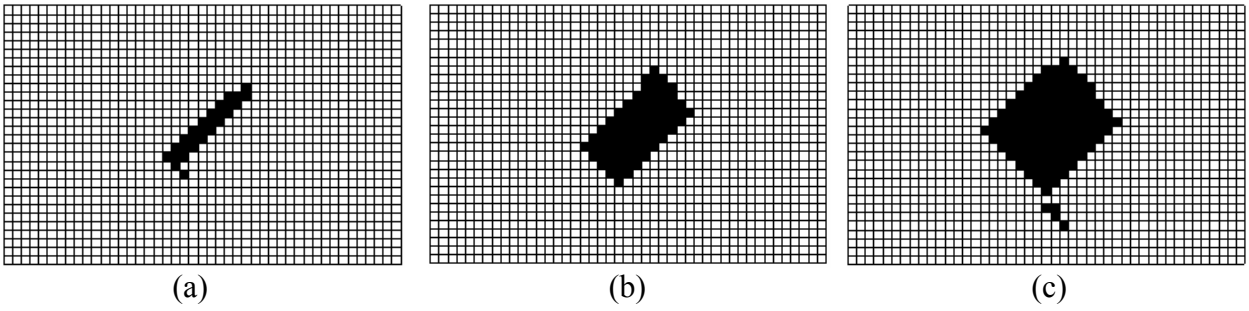

Figure 11: (a) 2% (b) 6% and (c) 10% treatment coverage for Mode 1 (first torsion mode), obtained using CA-4

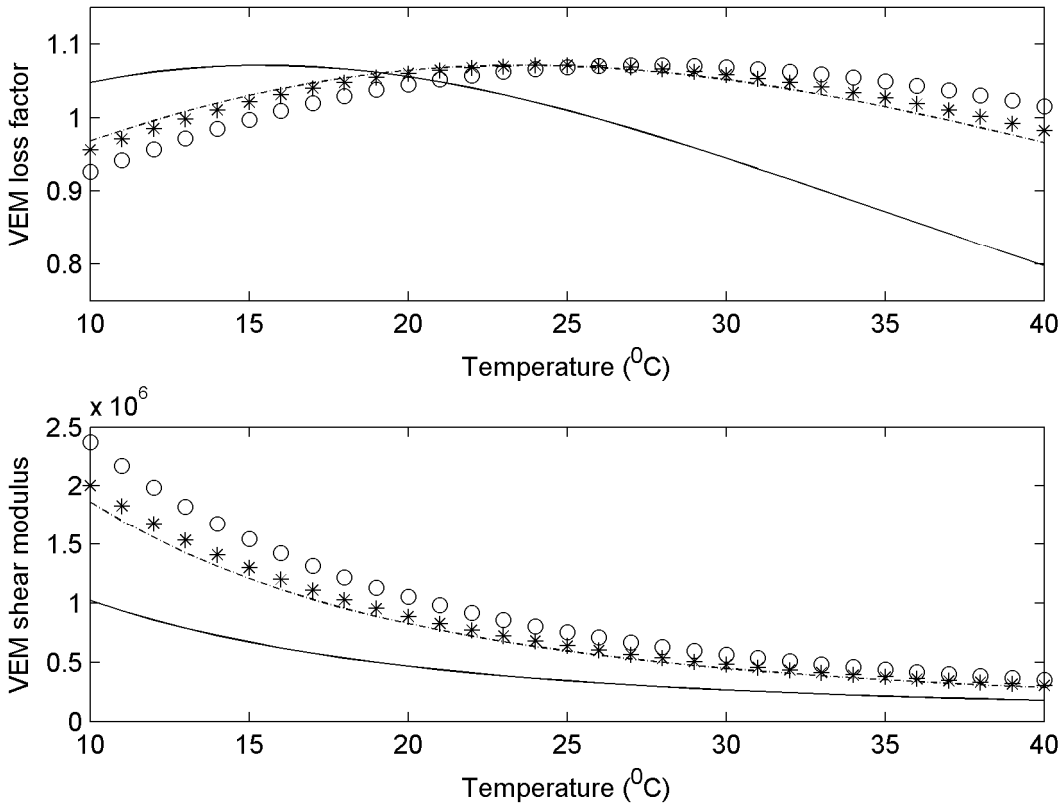

Figure 12: Complex modulus of ISD 112 at different frequencies and temperatures (solid line – Mode 1 (19.0Hz); dashed line – Mode 2 (60.5 Hz); stars – Mode 3 (71.4 Hz); circle – Mode 4 (96.1 Hz))

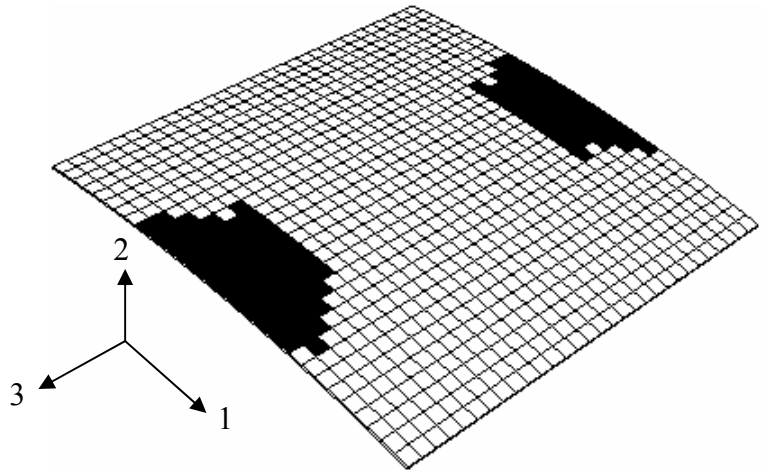

Figure 13: Treatment coverage obtained using CA-4 for curved panel, with identical weighting parameter over the 4 modes

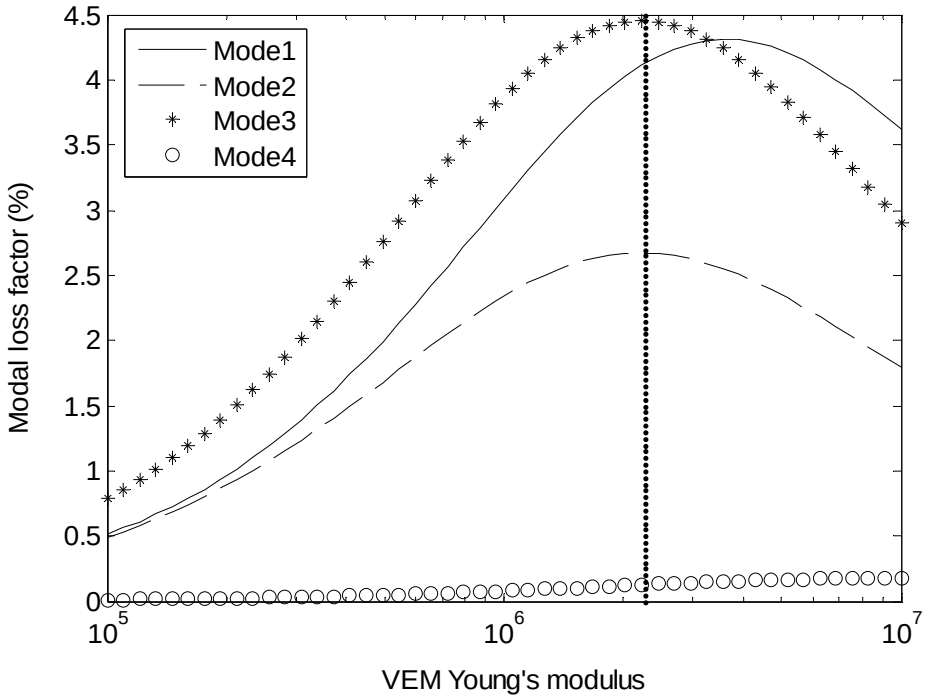

Figure 14: Plot showing damping performance of CLD curved panel of Figure 13 against the VEM stiffness (average VEM stiffness = 2.27 MPa at 21°C)

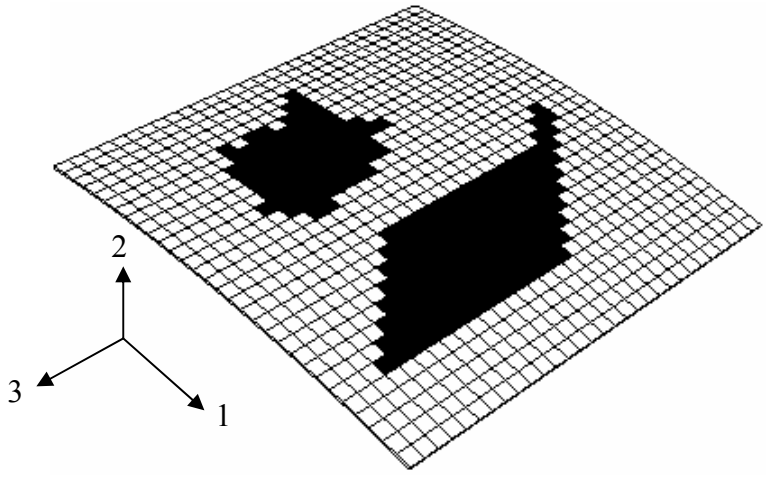

Figure 15: Treatment coverage obtained using CA-4 for curved panel, with the weighting parameter of the weakest mode set to unity

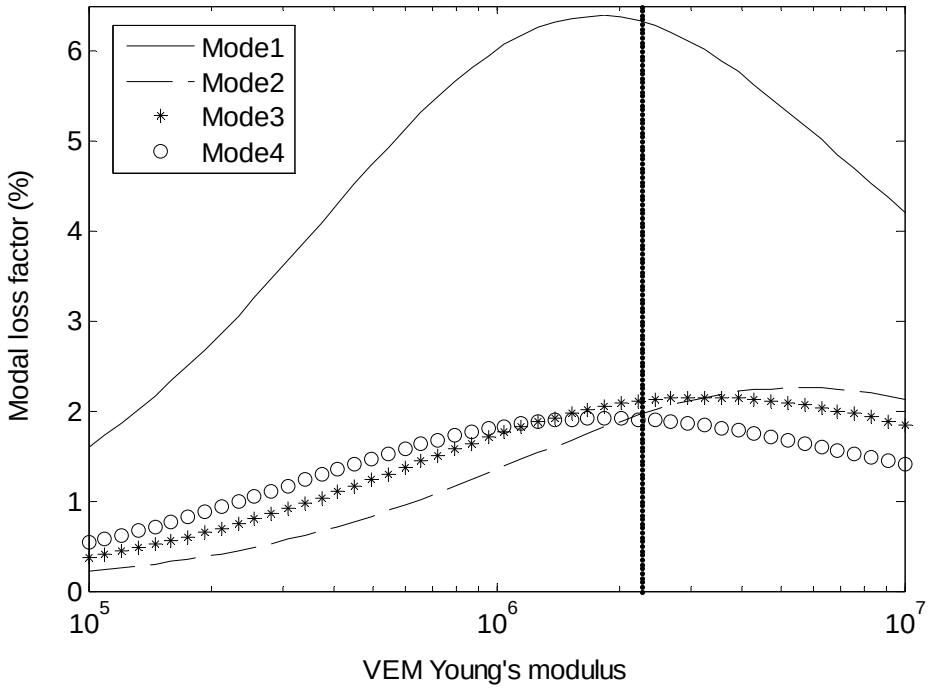

Figure 16: Plot showing damping performance of CLD curved panel of Figure 15 against the VEM stiffness (average VEM stiffness = 2.28 MPa at 21°C)

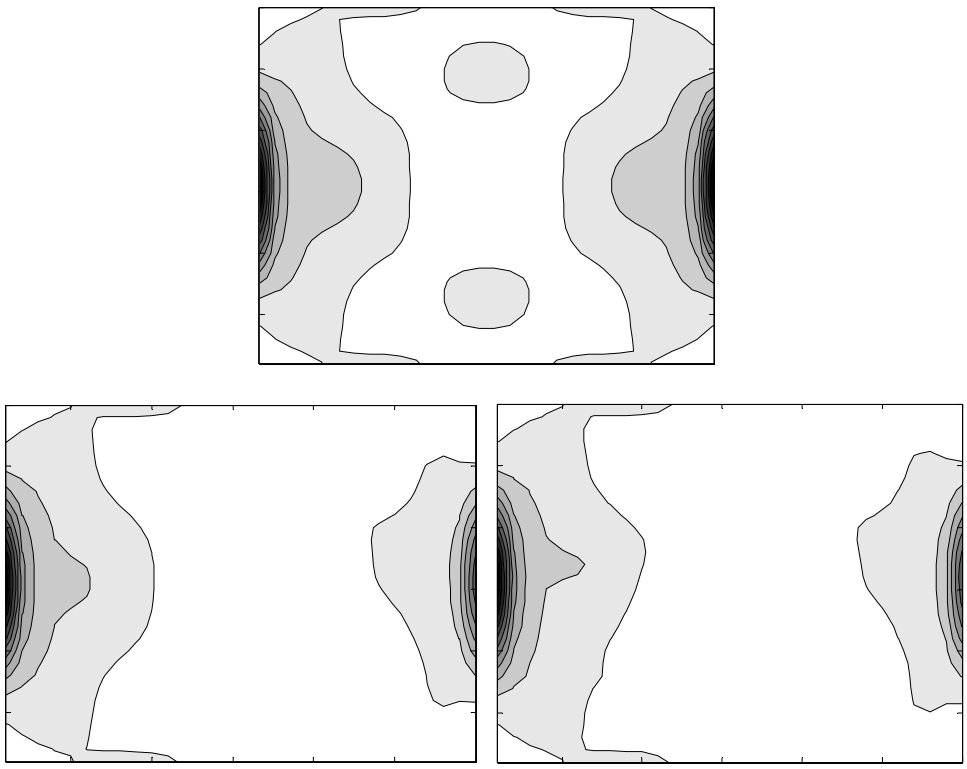

Figure 17: Contour plot of SED (heavy shading indicates high SED) on the curved composite panel for Mode 4 with (a) empty coverage (b) one and (c) two optimised patch obtained from "weakest mode' weighting parameter

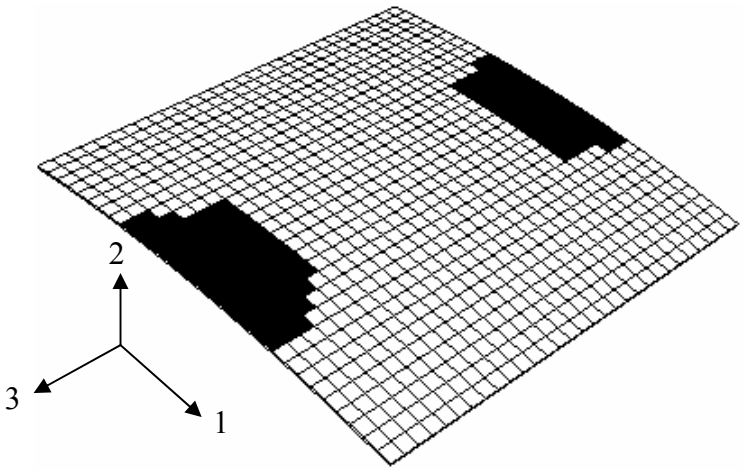

Figure 18: Treatment coverage obtained using CA-4 for curved panel, after smoothing procedure with identical weighting parameter over the 4 modes

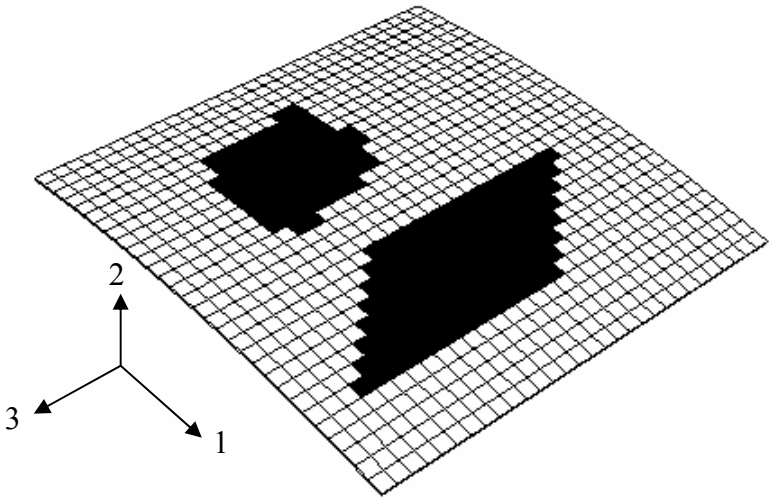

Figure 19: Treatment coverage obtained using CA-4 for curved panel, after smoothing procedure with the weighting parameter of the weakest mode set to unity

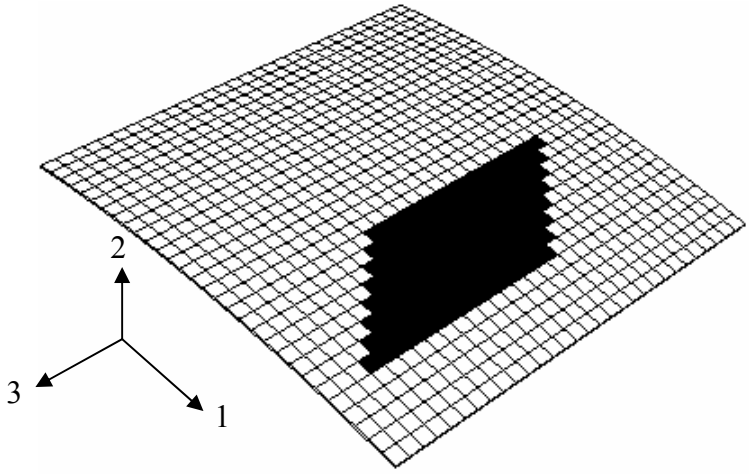

Figure 20: First patch obtained using CA-4 for curved panel, after smoothing procedure with the weighting parameter of the weakest mode set to unity

Figure 21: Experiment set up for CLD curved panel

Measured	Predicted
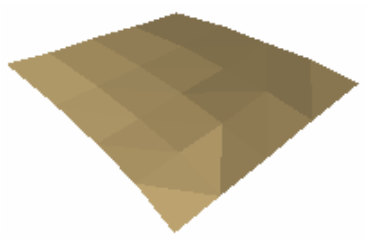	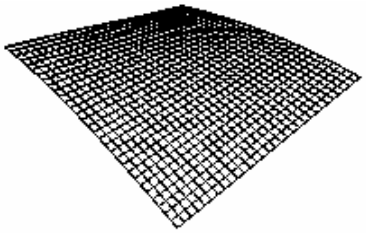
	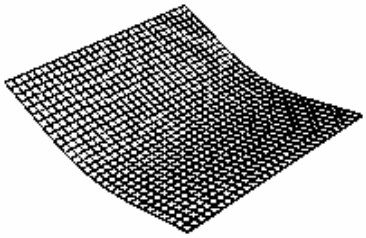
	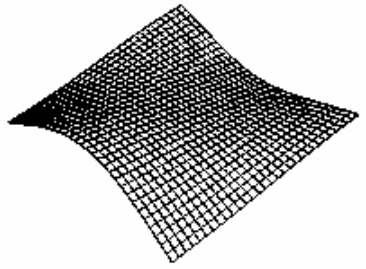
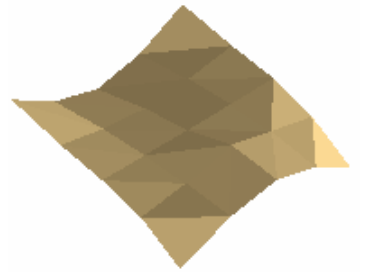	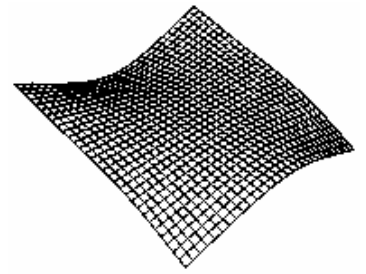

Figure 22: Mode shapes for first four modes of the untreated panel

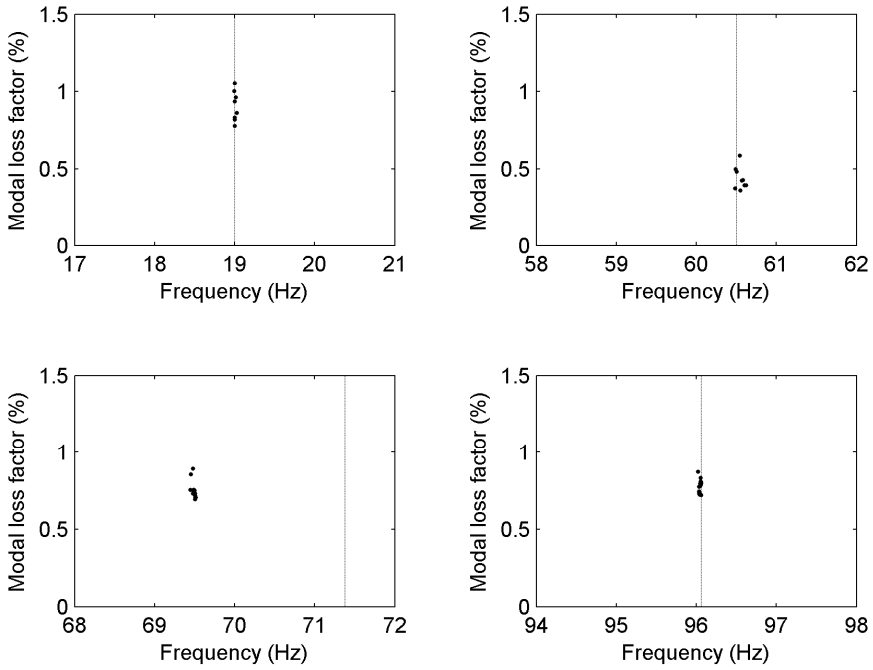

Figure 23: Plot showing the FE predictions (line) on the resonance frequency and the experimental measurements (dot) on both the resonance frequency and its modal loss factor, for untreated curved panel

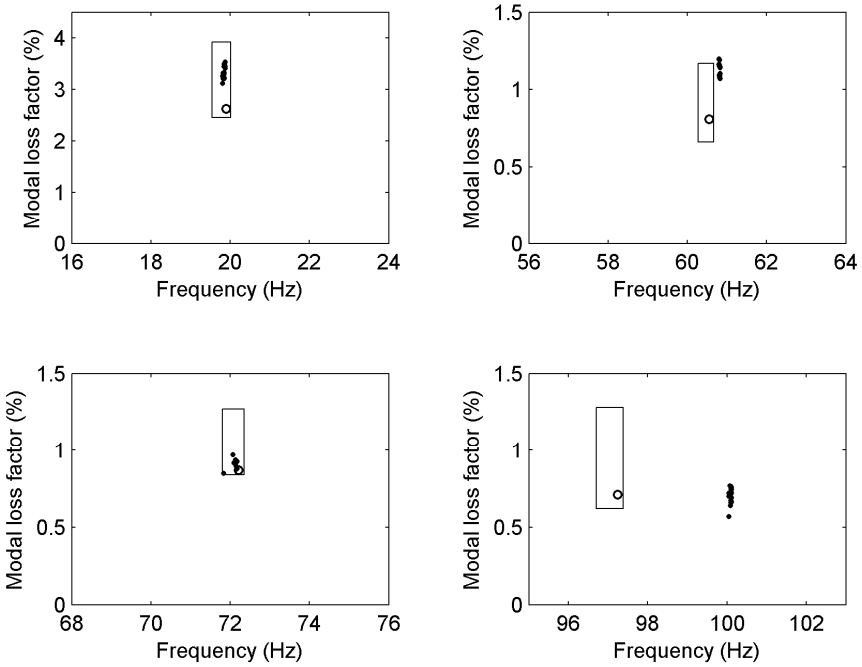

Figure 24: Plot showing the resonance frequency and its modal loss factor measured by LMS system (dot); predicted by MMSE (circle)using the average VEM Young's modulus at 23°C; upper and lower bound (square) predicted using both the MSE and MMSE method with temperature varying from 22–24°C

Tables

	Host structure	Damping layer (DL)	Constraining layer (CL)
Young's modulus	70GPa	8.7MPa	70GPa
Density	2700 kgm^{-3}	1100 kgm^{-3}	2700 kgm^{-3}
Poisson's ratio	0.3	0.45	0.3
Loss factor	0	0.3	0
Thickness	3mm	0.25mm	0.3mm
Width	300mm	Refer to Fig. 4 – 9 & 11	
Length	450mm		

Table 1: Dimensions and properties for the flat plate and the CLD treatments applied

Approach used	Loss factor ratio per unit added mass at 10% coverage		Approximate computational time on a Pentium(R) 4 CPU, with 3.2GHz and 1GB of RAM
	Mode 1	Mode 2	
CA-1	0.1889 (Fig. 4)	0.3615 (Fig. 5)	1 hour
CA-2	0.2995 (Fig. 6)	1.3477 (Fig. 7)	10 hours
Modified CA-2	0.4885 (Fig. 8)	1.3477 (Fig. 7)	10 hours
CA-3	0.7739 (Fig. 9)	1.3477 (Fig. 7)	1 – 3 hours
CA-4	0.8751 (Fig. 11)	1.3477 (Fig. 7)	10 hours

Table 2: Damping effectiveness for CLD obtained from different the CA algorithms

	Host structure	DL	CL
Young's modulus	E_1 = 20GPa E_2 = 88.385GPa E_3 = 52.675GPa	$E = G(2(1+2v))$	210GPa
Shear modulus	G_{12} = 4GPa G_{13} = 4GPa G_{23} = 7.944GPa	Refer to Fig. 12	65.625GPa
Poisson's ratio	v_{12} = 0.3 v_{13} = 0.3 v_{23} = 0.071	0.49	0.3
Density	1758 kgm^{-3}	1000 kgm^{-3}	7800 kgm^{-3}
Loss factor	0	Refer to Fig. 12	0
Thickness (1-direction)	3 mm	0.127 mm	0.18 mm
Length (2-direction)	600 mm	Refer to Fig. 13 – 20	
Width (3-direction)	600 mm		

Table 3: Dimensions and properties for the curved panel and the CLD treatments applied

Figure	Area coverage of the panel	Modal loss factor (%) (MSE)			
		Mode 1	Mode 2	Mode 3	Mode 4
13	13.1 %	4.13	2.67	4.45	0.13
15	22.2 %	6.32	1.97	2.11	1.90
18	13.2 %	4.17	2.70	4.41	0.11
19	21.5 %	6.31	1.93	2.09	2.03
20	13.3 %	3.92	1.10	1.26	1.11

Table 4: Modal loss factor obtained from different weighting parameter on curved panel